Sorting in early endosomes reveals connections to docking- and fusion-associated factors

Sina V. Barysch[a], Shweta Aggarwal[b], Reinhard Jahn[a,1], and Silvio O. Rizzoli[b]

[a]Department of Neurobiology, Max Planck Institute for Biophysical Chemistry, Am Fassberg 11, Göttingen 37077, Germany; and [b]European Neuroscience Institute, Grisebachstrasse 5, Göttingen 37077, Germany

Edited by Pietro V. De Camilli, Yale University School of Medicine, New Haven, CT, and approved April 24, 2009 (received for review February 9, 2009)

The early endosomes constitute a major sorting platform in eukaryotic cells. They receive material through fusion with endocytotic vesicles or with trafficking vesicles from the Golgi complex and later sort it into budding vesicles. While endosomal fusion is well understood, sorting is less characterized; the 2 processes are generally thought to be effected by different, unrelated machineries. We developed here a cell-free assay for sorting/budding from early endosomes, by taking advantage of their ability to segregate different cargoes (such as transferrin, cholera toxin subunit B, and low-density lipoprotein, LDL) into different carrier vesicles. Cargo separation required both carrier vesicle formation and active maturation of the endosomes. Sorting and budding were insensitive to reagents perturbing clathrin coats, coatomer protein complex-I (COPI) coats, dynamin, and actin, but were inhibited by anti-retromer subunit antibodies. In addition, the process required Rab-GTPases, phosphatidylinositol-3-phosphate, and, surprisingly, the docking factor early endosomal autoantigen 1 (EEA1). Sorting also required the function of the *N*-ethylmaleimide-sensitive factor (NSF), a well-known fusion cofactor, while it did not depend on preceding fusion of endosomes. We conclude that fusion, docking, and sorting/budding are interconnected at the molecular level.

budding | EEA1 | in vitro | NSF | SNAREs

Early endosomes represent major sorting platforms in eukaryotic cells. They constitute the first endocytotic compartment on which recently internalized vesicles converge, while they also receive carrier vesicles from the Golgi complex. Outgoing trafficking pathways include direct recycling of receptors to the plasma membrane, transport of elongated tubulo-vesicular structures to the recycling endosome, delivery of vesicles to the Golgi apparatus (involving the retromer complex), and finally maturation of early endosomes into multivesicular bodies/late endosomes that then fuse with lysosomes as the final destination. All incoming vesicular carriers join the endosomal compartment by membrane fusion. Conversely, all outgoing trafficking pathways involve the formation of carrier vesicles that bud from early endosomes (with the exception of traffic to late endosomes, which involves organelle maturation and invagination of vesicles).

In recent years, fusion (and the preceding step of docking) has been thoroughly described. Rab5 and its effectors (such as the class III phosphatidylinositol-3 (PI3)-kinase or the early endosomal autoantigen 1, EEA1), and soluble *N*-ethylmaleimide-sensitive factor (NSF) attachment receptors (SNAREs) and NSF itself, have been identified as key players in these processes (1, 2). In contrast, much less is known about the protein machineries involved in cargo sorting and vesicle budding from early endosomes.

One of the reasons for this gap in our knowledge is that, in contrast to fusion (3, 4), it has been difficult to reconstitute sorting from endosomes in vitro. Compared to live cell approaches, in vitro assays allow direct biochemical access to the docking and fusion machineries (for instance, proteins can be depleted or perturbed using cell-impermeant inhibitors such as antibodies). Sorting and formation of vesicular carriers from early endosomes have so far been largely studied in live cells using approaches such as electron microscopy (5) or monitoring transferrin release from intact cells (6–8). There is so far no convenient and sensitive assay available for monitoring these processes in vitro although several lines of evidence document that budding of vesicles from endosomes can occur under cell-free conditions (9–11).

In the present study, we have developed a novel microscopy-based cell-free assay for early endosomal segregation of cargo. We took advantage of the fact that transferrin (as a recycling marker) and low-density lipoprotein (LDL) (as a marker for the degradative pathway) are differentially sorted within early endosomes. We show here that isolated endosomes double labeled with fluorescent transferrin and LDL efficiently separated these 2 markers in vitro, a process that turned out to be rather easy to monitor and quantify. Surprisingly, we found that the docking factor EEA1 and the fusion cofactor NSF (the ATPase that disassembles SNAREs), but not fusion itself, are required for sorting and budding of recycling vesicles. Importantly, these conclusions are not restricted to the differential sorting of transferrin and LDL, as cholera toxin/LDL sorting also depended upon the same factors. Our results therefore suggest an unexpected connection between docking/fusion and sorting/budding at the molecular level.

Results

Characterization of an in Vitro Microscopy-Based Assay for Early Endosomal Sorting. For the establishment of a budding assay from early endosomes, we used PC12 cells, a neuroendocrine cell line. Like many mammalian cells, PC12 cells rapidly recycle transferrin, while they target LDL for degradation. PC12 cells were incubated for 5 min with fluorescent transferrin (Alexa 488) and LDL (DiI). As expected, PC12 cells endocytose large amounts of both LDL and transferrin (Fig. 1*A*), with a substantial fraction of the organelles being double labeled. After a chase period the amount of double-labeled organelles is drastically reduced (but not eliminated, see Fig. 1*B* for quantification), mainly through transferrin recycling (note the strong decrease in transferrin signal after the chase, Fig. 1*A*).

To allow easier manipulations of the sorting process, we proceeded to reproduce it in an in vitro assay. We prepared postnuclear supernatants (PNS) from cells labeled with both endocytotic tracers (see schematic in Fig. 1*C*). We then incubated the PNS at 37 °C (or kept it on ice as a negative control) in a reaction mixture containing rat brain cytosol and an ATP-regenerating system and measured the amount of double-labeled organelles using fluorescence microscopy. The number of double-labeled organelles was in line with the observations from living cells, with ≈15–30% of all LDL-

Author contributions: S.V.B. and S.O.R. designed research; S.V.B. and S.A. performed research; R.J. and S.O.R. contributed new reagents/analytic tools; S.V.B., S.A., and S.O.R. analyzed data; and S.V.B., R.J., and S.O.R. wrote the paper.

The authors declare no conflict of interest.

This article is a PNAS Direct Submission.

Freely available online through the PNAS open access option.

[1]To whom correspondence should be addressed. E-mail: rjahn@gwdg.de.

This article contains supporting information online at www.pnas.org/cgi/content/full/0901444106/DCSupplemental.

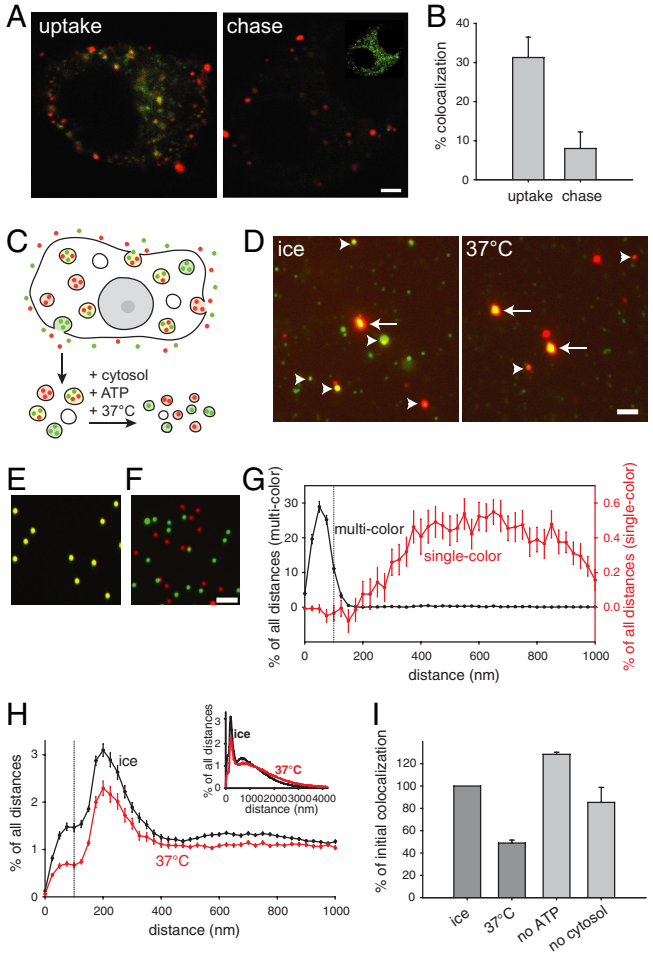

Fig. 1. The microscopic assay for early endosomal sorting. (*A*) Segregation of labeled cargo in vivo. PC12 cells were loaded simultaneously with transferrin (green) and LDL (red) for 5 min (*Left*). During a chase period of 30 min (*Right*), a substantial amount of the transferrin is released from the cells, thus clearly segregating from the LDL label, which remains trapped. However, some transferrin still persists within intracellular organelles (see inset; the chased cell is depicted with increased contrast). (*B*) Quantification of colocalization in vivo. Approximately 30% of the organelles were initially double labeled, decreasing to ≈8% after the chase. Bars show means ± SEM ($n = 3$). (*C*) Schematic overview of the in vitro sorting assay. PC12 cells are loaded simultaneously with labeled transferrin (green) and LDL (red), and postnuclear supernatant (PNS) is prepared. Incubation of the PNS in the presence of ATP and cytosol results in separation of the 2 labels due to budding. (*D*) Fluorescence images from samples incubated on ice (negative control) and samples incubated at 37 °C (positive control). Images acquired in the green (transferrin) and red (LDL) channels were aligned by using fluorescent beads (arrows) as a reference. Many endosomes appear initially (on ice) double labeled (yellow, arrowheads). After sorting, less colocalized (i.e., double-labeled) spots are visible. (Scale bar, 2 μm.) (*E–G*) Typical images from multicolored (*E*) or single-colored (*F*) fluorescent beads. Images acquired in the green and red channels were aligned (see *SI Methods*), intensity centers from all of the spots (beads) in both the green and red channels were calculated, and the distance from each spot to the closest one in the other channel was measured and plotted in a histogram (*G*). While the distance between single-colored objects never falls below about ≈200 nm, virtually all double-labeled beads have their green and red intensity centers within a 100-nm distance (vertical dotted line). The graph shows means ± SEM ($n = 3$). (*H*) The same measurements as in *G* were performed with transferrin- and LDL-containing early endosomes before (ice, black curve) and after (37 °C, red curve) the sorting reaction. The amount of double-labeled organelles (± SEM ($n = 43$). Note that, for clarity, the plot shows distances only up to 1000 nm (full-scale graph shown as inset). (*I*) Quantification of colocalization. We measured the percentage of organelles that have their green and red intensity centers within 100 nm. Colocalization decreases by 50% after the sorting reaction (initial colocalization refers to samples incubated on ice). Removal of ATP or omission of cytosol completely blocks this reaction. Bars show means ± SEM ($n = 4$).

containing organelles being colabeled with transferrin (which, as more organelles were labeled with transferrin, translated into 2–6% of all transferrin-containing organelles being colabeled in independent PNS preparations). Also, just as in the cellular context, the amount of double-labeled organelles dropped substantially (but did not disappear) after incubation (compare the 2 panels in Fig. 1*D*), allowing us to conclude that the in vitro sorting reaction faithfully follows the in vivo situation.

Control experiments were then carried out to ensure that the decrease in the number of double-labeled organelles is because of sorting and budding, instead of representing the breakup of aggregates containing red and green endosomes, or the degradation (or leakage) of the endocytosed label [see supporting information (*SI*) Fig. S1]. We have recently demonstrated that we can discriminate between docked (clustered) and genuinely double-labeled endosomes in a similar fluorescence-based assay (12). Briefly, to quantify the degree of colocalization, we measured the distances between the intensity centers of the green and red spots and recorded for each green spot the distance to its closest red neighbor. When applied to fluorescent beads of endosome size (≈200 nm in diameter; Fig. 1 *E* and *F*), this method demonstrated that the green and red centers of a multicolor bead are within 75–100 nm from each other, while 2 differently colored beads cannot get closer to each other than ≈150–200 nm (Fig. 1*G*). Thus, we can safely assume that endosomes whose green and red intensity centers are within ≈100 nm from each other are indeed double labeled (see also ref. 12 for further controls).

In endosomes from PC12 cells labeled with transferrin and LDL (Fig. 1*H*) a fraction of the organelles were clearly double labeled, with their intensity centers being closer than 100 nm to each other (Fig. 1*H*, vertical dotted line). A second peak was observed at a distance of around ≈200 nm, probably reflecting docked endosomes. Incubation at 37 °C reduced the relative amount of both pools, with the proportion of double-labeled endosomes being reduced substantially (Fig. 1*H*, red line). To quantify the separation of fluorescent markers under different conditions, we determined the fraction of double-labeled objects in relation to all green (transferrin)-labeled objects. Incubation reduced colocalization by 50%, in an ATP- and cytosol-dependent manner (Fig. 1*I*), as one would expect for a sorting reaction.

We expected that other cargoes would also be efficiently separated in vitro. This was indeed the case, with a number of cargoes separating well from each other: acetylated LDL from transferrin, LDL from cholera toxin B (a molecule known to traffic through endosomes to the Golgi apparatus), or the inert label dextran from transferrin. Importantly, we detected no significant separation when using a mixture of green- and red-labeled transferrin (Fig. S2).

Finally, one possible complication of this assay is that the newly budded vesicles could in principle fuse with each other. Therefore, we checked the fusion rates between the different cargoes (Fig. S3). As expected, LDL-containing vesicles fused very poorly with transferrin-containing ones (as did also LDL- and cholera toxin-labeled vesicles).

In Vitro Sorting Does Result in the Formation of Small Transferrin-Containing Vesicles. While the assay we presented clearly results in the separation of transferrin and LDL from endosomes, it is still an open question whether it does so by physiological mechanisms—i.e., by the budding of small transferrin-containing vesicles.

We used a number of different methods to check this. First, we observed that, in addition to the decrease in colocalization, transferrin-, cholera toxin-, and dextran-containing organelles seemed to become less bright upon incubation (Fig. S4), indicative of budding of (small) vesicles from the endosomes. Not to rely only on separate samples incubated under different conditions, we also monitored individual endosomes over time. We adsorbed labeled organelles containing transferrin and LDL to coverslips before adding the cytosol–ATP mixture in a temperature-controlled microscopy in-

cubation chamber. While transferrin-containing endosomes lost a substantial fraction (but not all) of their initial fluorescence, again indicative of budding of small transferrin-containing vesicles, LDL-containing organelles did not get dimmer (compared to the bleaching control), exactly as one would expect (Fig. S5).

Second, as these measurements cannot give an indication of the vesicle size (with most organelles being smaller than the diffraction limit), we also used a diffraction-unlimited fluorescence microscopy technique, stimulated emission depletion (STED) (13). Cells were labeled with transferrin coupled to a STED-efficient dye, Atto 647N. The size of the transferrin-containing organelles dropped significantly after incubation both in living cells and in vitro (Fig. 2 *A* and *C*). Note also that the vesicle sizes (both before and after incubation) were similar in living cells and in vitro (Fig. 2 *B* and *D*), as expected. As independent confirmation, a very similar size reduction after incubation was observed by electron microscopy, using endosomes preloaded with horseradish peroxidase (HRP) as a fluid phase marker (Fig. S6).

Third, we used differential centrifugation to examine whether endosomes can be separated from small transferrin-containing transport vesicles. Endosomes were labeled with HRP or transferrin–Alexa 488. First, slow speed centrifugation was carried out to sediment larger (not budded) endosomes. The small vesicles remaining in the supernatant were then collected by high-speed centrifugation (Fig. 2*E*). The HRP content in the high-speed pellet was measured by a colorimetric reaction, while transferrin was quantified by immunoblotting with anti-Alexa 488 antibodies. In the presence of ATP, a major increase of the recycling markers was observed (Fig. 2 *F* and *G*).

Thus, the assays used here concur in suggesting that small vesicles containing transferrin form from the double-labeled endosome precursors.

Fusion/Docking Factors Are Involved in Early Endosomal Sorting. We next proceeded to characterize the sorting and segregation reaction, using the assay described in Fig. 1. The reaction followed an exponential curve with a half time of 11.5 min (Fig. 3), basically identical to what we observed in living cells (Fig. S7).

In view of the almost universal involvement of GTPases in the secretory pathway, it was not surprising that GTPγS or GMP-P(NH)P reduced the sorting reaction by ≈50%. In contrast, other treatments proposed to interfere with endosome function in the past, such as chelating calcium ions, disturbing the proton gradient, or perturbing cytoskeletal elements, had no measurable effects (Fig. 3*B*). More interestingly, transferrin/LDL segregation was strongly inhibited by the phosphatidylinositol-3-kinase (PI3K) inhibitor wortmannin (Fig. 3*B*), with an IC_{50} of ≈15.6 nM (Fig. S8), which is consistent with previous findings (6, 7), and by the PI3K inhibitors LY 294,002 and 3-Methyladenine.

PI3P serves as coincidence detector in recruiting Rab5-effectors such as the EEA1, and PI3K inhibition releases EEA1 from the endosome membrane in our assay (data not shown). Therefore, we tested whether EEA1 is involved not only in membrane tethering and fusion, but also in sorting/budding. As shown in Fig. 4*A* (*Upper*), a polyclonal antibody against the N-terminal peptide of EEA1 fully blocked segregation of transferrin and LDL (the effect was eliminated by addition of the antigenic peptide). The budding reaction also depended upon Rab GTPases, as observed from the strong block caused by addition of GDP dissociation inhibitor (GDI), which strips Rab proteins from the membrane. Interestingly, the effects of wortmannin, GDI, and the EEA1 antibody on sorting and budding were much stronger than on endosome fusion, which was inhibited only by 15–30% under our experimental conditions (Fig. 4*A*, *Lower*).

The data shown so far indicate that segregation is sensitive to interference with proteins that are rather known to act in docking and fusion. The question arises whether these proteins function in sorting/budding independent of fusion or whether

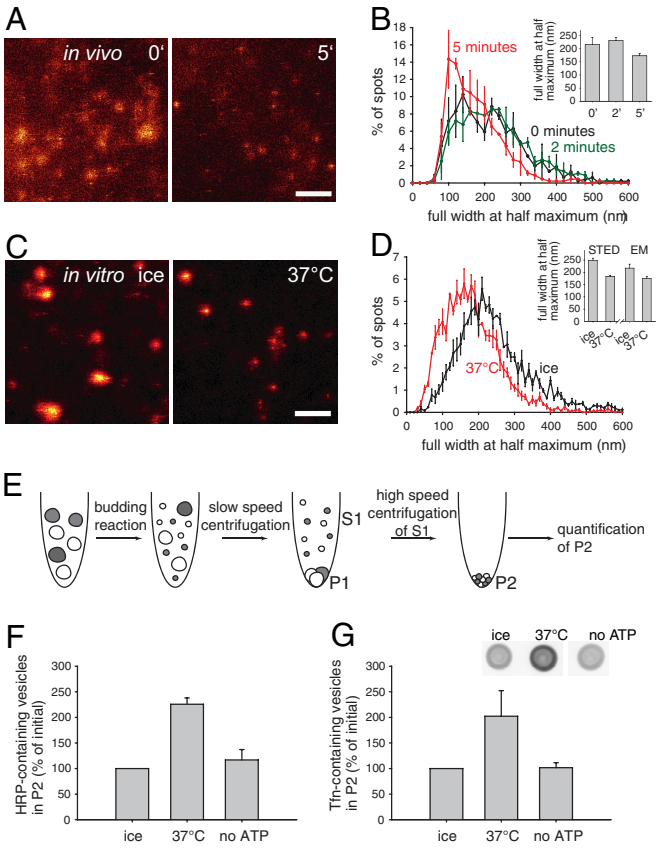

Fig. 2. In vitro sorting results in the formation of small transferrin-containing vesicles. (*A*) STED microscopy images of PC12 cells labeled with transferrin–Atto647N. Cells were allowed to bind and internalize transferrin for 15 min on ice. After washing the unbound transferrin, cells were chased for different time periods (0, 2, and 5 min) at 37 °C. After 5 min of chase, organelles appear smaller compared to the initial situation. (Scale bar, 1 μm.) (*B*) Size distribution of transferrin-containing endosomes in vivo as determined by STED microscopy. We measured the sizes from 600-1000 organelles per condition per experiment by taking line scans, fitting Lorentzian curves, and calculating the full width at half maximum (see *SI Methods*). A bar graph with the average sizes for each condition (inset) and a histogram with 20-nm bins show a decrease in the size of organelles after 5 min. Bars show means ± range of values ($n = 2$). (*C*) STED microscopy images of endosomes labeled with transferrin–Atto647N before (ice) and after the in vitro sorting reaction (37 °C). Endosomes appear initially much bigger than after the reaction. (Scale bar, 1 μm.) (*D*) Size distribution of transferrin-containing endosomes in vitro as determined by STED microscopy. We measured the sizes from 600-1000 organelles per condition per experiment as in *B*. A bar graph with the average sizes for each condition (inset) and a histogram with 10-nm bins show a decrease in the size of transferrin-containing organelles after the reaction. Bars show means ± SEM ($n = 3$). For comparison, the inset also shows the endosome size change in HRP-labeled endosomes, investigated by electron microscopy (means ± range of values, $n = 2$; see also Fig. S6). Note that the graph plots the full width at half maximum for the fluorescence data and the diameter for the electron microscopy data. (*E*) To investigate whether our in vitro sorting reaction results in budding of small vesicles, we established a biochemical budding assay (see schematic overview). A typical reaction was performed with HRP- or transferrin–Alexa 488-containing endosomes. To separate small vesicles from larger organelles, we performed a slow-speed centrifugation step. The supernatant containing the small vesicles was then subjected to a high-speed centrifugation, which ensured that we pelleted all remaining membranes in the pellet P2. The amount of newly formed small vesicles in P2 was then analyzed by an HRP-colorimetry reaction or by blotting for transferrin–Alexa 488 (see below). (*F*) Quantification of HRP-containing vesicles from P2 by a colorimetric ABTS reaction. Bars show means ± SEM ($n = 6$). (*G*) Quantification of small, transferrin–Alexa 488-containing vesicles from P2 by dot blots stained with antibodies against Alexa 488 (inset). Bars show means ± SEM ($n = 4$–5). Note that in both of the biochemical assays, the amount of small vesicles increases with budding, in an ATP-dependent manner.

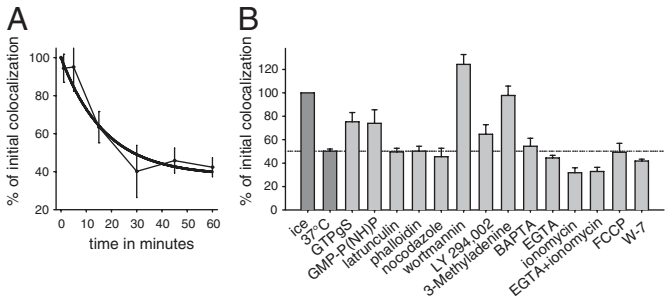

Fig. 3. Requirements of the sorting reaction. (*A*) Time course of the sorting reaction. The graph shows means ± range of values (n = 2–3); the solid line represents an exponential decay fit. (*B*) Effects of different reagents on early endosomal sorting of cargo: GTPγS (200 μM), GMP-P(NH)P (1 mM), latrunculin (15 μM), phalloidin (10 μM), nocodazole (20 μM), wortmannin (50 nM), LY 294,002 (100 μM), 3-Methyladenine (5 mM), BAPTA (10 mM), EGTA (10 mM), ionomycin (10 μM), FCCP (50 μM), and W-7 (100 μM) were added. The PI3K inhibitors block the reaction significantly. Bars show means ± SEM (n = 3–10).

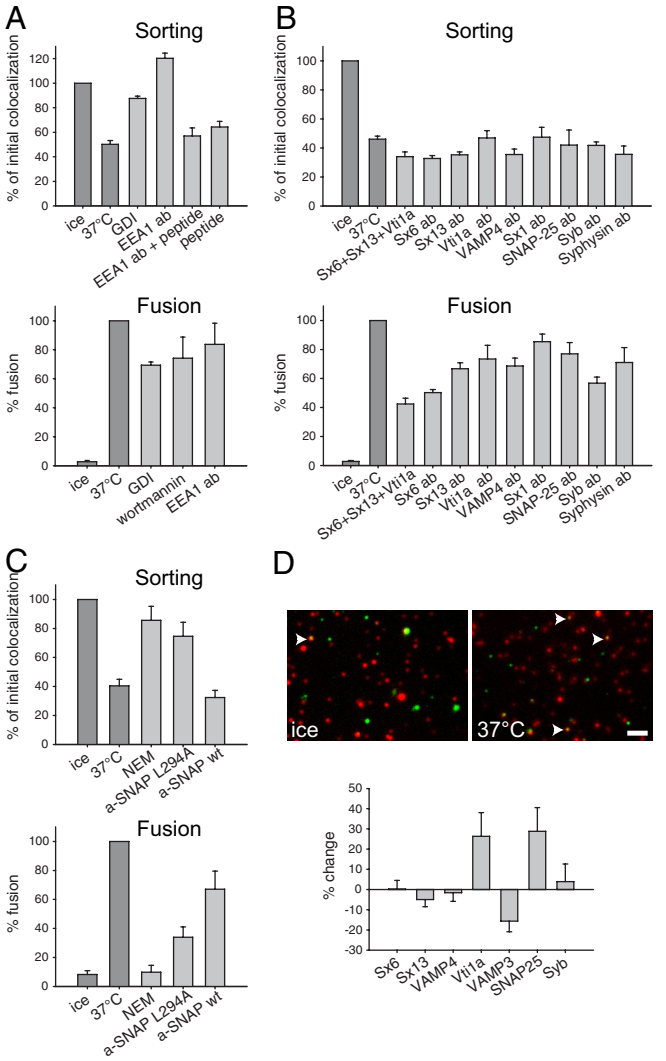

Fig. 4. Fusion/docking factors, but not the fusion step itself, are essential for sorting in early endosomes. (*A*) Sorting reactions (*Upper*) were performed as above. The indicated reagents were added (10 μM GDI, polyclonal antibodies against the N-terminal peptide of EEA1, 200 μM of antigenic peptides, and 50 nM wortmannin). In vitro fusion reactions (see *SI Methods*) were performed in parallel to check the effect of these reagents on the fusion (*Lower*). While GDI and the antibodies block cargo separation completely, they have only a minor effect on fusion. Bars show means ± SEM (n = 3–6 for sorting, n = 3 for fusion). (*B*) Addition of the recombinant cytosolic SNARE fragments syntaxin 6, syntaxin 13, and vti1a (30 μM each) or several polyclonal sera against SNAREs inhibits fusion efficiently (*Lower*) although they have no effect on cargo separation (*Upper*). Bars show means ± SEM (n = 3 for sorting and n = 4–5 for fusion). (*C*) Both *N*-ethylmaleimide (NEM, 2 mM) and the dominant-negative mutant of the NSF cofactor α-SNAP (L294A, 50 μM) block budding and fusion while the wild-type α-SNAP (50 μM) has no effect. Bars represent means ± SEM (n = 4–10 for sorting and n = 5–9 for fusion). (*D*) Immunostainings of transferrin–Alexa 488-containing organelles (green) before and after sorting. We centrifuged the endosomes onto coverslips and immunostained them with antibodies against vti1a (*Upper*) or syntaxin 6 (Sx6), syntaxin 13 (Sx13), VAMP4, VAMP3, synaptobrevin (Syb), and SNAP-25. Thirty percent to 70% of the organelles were positive for each of the SNAREs (data not shown). Arrowheads show colocalized organelles. Bars show the change in colocalization after budding for the respective SNAREs (means ± SEM, n = 3–6). (Scale bar, 2 μm.)

fusion is a prerequisite for budding. Therefore, we tested whether budding is also dependent on the function of SNARE proteins that catalyze fusion. We used soluble recombinant SNARE fragments (as competitive inhibitors) and anti-SNARE antibodies to interfere with SNARE function. In agreement with previous observations (4), all of these reagents inhibited fusion (albeit to a different extent, ranging from 15% to 60%), but none inhibited sorting/budding (Fig. 4*B*).

We then analyzed whether the sorting reaction is dependent on the activity of the *N*-ethylmaleimide (NEM)-sensitive factor (NSF). NSF, together with its cofactor α-SNAP, is required for all fusion steps in the secretory pathway. NSF functions by dissociating SNARE complexes, keeping the SNAREs in a "ready for fusion" state. When NSF is inhibited, fusion stops rapidly, as most available SNAREs on the endosome membrane spontaneously form stable 4-helical SNARE complexes (14). NEM, a potent, but nonspecific, NSF inhibitor blocked the sorting reaction (Fig. 4*C*) (10, 15). To test whether this was due to a specific block of NSF, we used a dominant negative variant of the cofactor α-SNAP [α-SNAP L294A (ref. 16)], which also blocked sorting; wild-type α-SNAP was, as expected, ineffective (Fig. 4*C*, *Upper*). These tools potently blocked fusion as well (Fig. 4*C*, *Lower*).

Why is NSF activity (Fig. 4*C*), but not SNARE function (Fig. 4*B*), required? One possibility is that SNARE-independent NSF effects are involved, although this is unlikely, because α-SNAP is known to function exclusively in SNARE regulation (17). Without NSF, the SNAREs form stable complexes on the endosomal membrane, which are entirely nonselective—any 4 compatible SNAREs will complex, irrespective of their function in different pathways (14). However, these complexes would need to be separated (via NSF), to allow for SNARE sorting and formation of newly budded vesicles, if the carrier vesicles have a different SNARE from the original organelles. This is indeed the situation: when we immunostained transferrin-positive organelles with antibodies against different SNAREs, before and after incubation (budding), substantial changes were seen in the SNARE makeover of the vesicles (Fig. 4*D*).

As the finding that docking and fusion factors function in sorting is largely unexpected, we decided to test them also in a second sorting reaction, such as cholera toxin/LDL sorting. To be able to compare directly this reaction to transferrin/LDL sorting, we used preparations labeled simultaneously with all 3 labels. A substantial fraction of the organelles were multiply labeled: 20.5 ± 0.9% of the LDL-labeled endosomes were positive for transferrin, 15.7 ± 0.7% were positive for cholera toxin, and 6 ± 0.4% were triple labeled (n = 7 independent experiments). As indicated in Fig. S9, cholera toxin/LDL behaved identically to transferrin/LDL sorting, with a clear dependence upon EEA1 and NSF, but not on SNARE function itself. Importantly, sorting of material from triple-labeled endosomes also exhibited the same characteristics (Fig. S9 *B* and *C*).

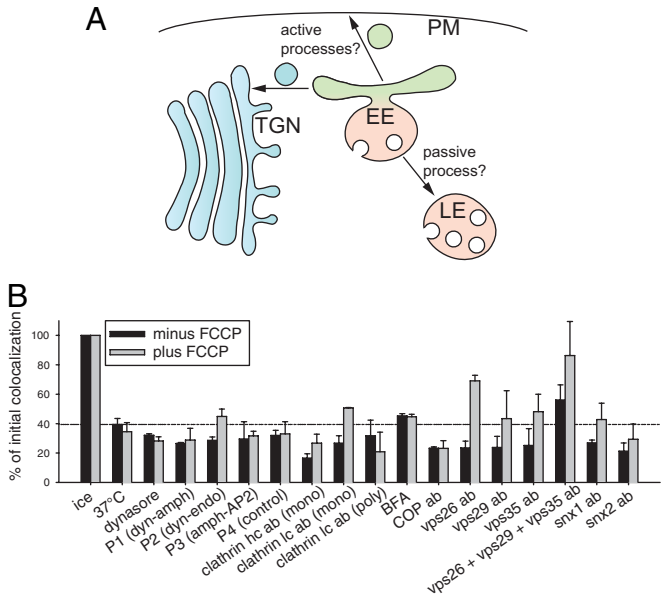

Fig. 5. Carrier vesicle formation and endosome maturation in cargo sorting. (*A*) Hypothetic model of cargo separation. Early to late endosome maturation may be either a passive or an active process, while cargo vesicle formation can only be seen as active. (*B*) Effects of different reagents on early endosomal sorting of cargo, both in the absence (black bars) and in the presence (gray bars) of 50 μM FCCP, using triple-labeled endosomes as in Fig. S9. The following reagents were used: dynasore (80 μM), peptides (1 mM for P1 and P2 and 100 μM for P3 and P4), brefeldin A (360 μM), and antibodies (1:16) were added. Bars show means from 2–3 independent experiments (±SEM; when only 2 experiments were performed, the range of values is shown instead).

Both Carrier Vesicle Formation and Endosome Maturation Are Required for Cargo Sorting. To identify some of the effectors involved in formation of new vesicles from the sorting endosomes, we proceeded to investigate the behavior of the triple-labeled endosomes in the presence of a number of inhibitory reagents for molecules proposed to function in budding reactions (Fig. 5*A*).

We used a number of tools directed against dynamin (the inhibitor dynasore and peptides perturbing its interaction with amphiphysin or endophilin), AP2/amphiphysin (peptide perturbing their interaction), clathrin light and heavy chain (antibodies targeting the 2 subunits), coatomer protein complex-I (COPI) coats (brefeldin A or antibodies against the EAGE-peptide of βCOP), sorting nexins 1 and 2 (antibodies), and the retromer subunits Vps26, Vps29, and Vps35 (antibodies) (Fig. 5*B*). Only a combination of the 3 anti-Vps antibodies resulted in mild inhibition (although all of these tools have been thoroughly described in the past; see *SI Text* for details and references).

One explanation for the limited inhibition we observed is that separation of cargoes requires not only the budding of transferrin or cholera toxin carrier vesicles, but also active maturation of the LDL-containing organelles (Fig. 5*A*). To block maturation, we inhibited the acidification of the triple-labeled organelles, using the proton gradient perturber carbonyl cyanide 4-(trifluoromethoxy)-phenylhydrazone (FCCP); this treatment alone is not sufficient to block cargo separation (see Fig. 3*C*). We next combined FCCP with the tools mentioned above (Fig. 5*B*, gray bars). Addition of FCCP to anti-retromer tools resulted in a strong inhibition of the reaction, while anti-clathrin/dynamin or COPI tools were still ineffective. Similar results were obtained when quantifying the separation of transferrin from LDL, or cholera toxin from LDL (data not shown), as was also the case for the conditions indicated in Fig. S9.

Discussion

In the present study we describe a cell-free assay for the sorting of recycling vesicles from early endosomes, which is based on fluorescence microscopy. The assay proved to be highly reliable and allowed for identifying some of the factors essential for this process, such as cytosol, an energy source, and major players in membrane sorting (such as PI3-kinases and Rab proteins). These findings are in line with results from other in vitro budding assays, such as those reconstituting the formation of secretory granules from the TGN (18), late endosome to Golgi transport (19), the formation of GLUT4 or transferrin receptor-containing endocytic small vesicles (ESVs) from early endosomes (20), or the formation of COPII coated vesicles from synthetic proteoliposomes (21). As expected, transferrin recycling proceeds through the formation of small vesicles from the endosomes, in agreement with previous biochemical in vitro budding assays (10, 11) performed in the same system (PC12 cells).

Our results suggest that in addition to formation of carrier vesicles, successful separation of the cargoes requires endosome maturation (i.e., acidification), although from a mechanistic standpoint it may have been more intuitive to see the maturation process as only passive. The nature of the molecules involved in carrier vesicle formation is still an open issue (see, for example, refs. 22 and 23), with the retromer complex being clearly involved [in agreement with results from the groups of Bonifacino (24) and Johannes (25), who suggested that small vesicles destined to the trans-Golgi network bud from the early endosome through retromer-dependent processes]. Surprisingly, we found that specific inhibition of the docking and fusion factors EEA1 and NSF leads to a block of cargo segregation. NSF activity, but not SNARE-mediated endosome fusion, was required for formation of recycling vesicles. Coupling this with the fact that the SNARE composition of transferrin-containing organelles changes after the reaction, one is tempted to conclude that SNARE separation and sorting into different compartments on the endosomal membrane are necessary for this process. This view is in agreement with previous findings showing that certain SNARE molecules can interact with coat proteins, which is likely important for SNARE sorting (26–31).

EEA1 is a molecule that has been described to operate downstream of Rab5 and the class III PI3-kinase VPS34 in organelle docking (32), although it has also been known for more than a decade that it also is a component of a multiprotein (and perhaps multifunction) machinery containing EEA1, NSF, and also Rab5 and endosomal SNAREs (syntaxin 6 or 13) (33–35). The fact that an antibody against EEA1 strongly blocks budding (even stronger than it blocks fusion) is difficult to reconcile with an exclusive function for this molecule in tethering of endosomes before the fusion event, although it is in line with a recent observation that EEA1 knockdown perturbs transferrin dynamics and epidermal growth factor processing (36). One possible explanation is that the processes of endosome docking/fusion and sorting/budding are linked, being performed by macromolecular machineries containing components involved in both processes. This is in line with observations on yeast vacuoles (the equivalent of mammalian late endosomes), where dynamin appears to be required not just for budding, but also for fusion (37). It is even possible that EEA1 perturbation results in a reduced activity of NSF (which would in itself block sorting). Taken together, our results are in line with a view of endosomal traffic in which the events of docking, fusion, and budding are tightly connected on a molecular level.

Methods

Materials, reagents, and previously published methods are described in detail in *SI Methods*.

Sorting Reaction. Reaction mixtures contained, as final concentrations, 4 mg/mL PNS (labeled with transferrin–Alexa 488, transferrin–Alexa 594, LDL-DiI, acetylated LDL–Alexa 594, dextran–Alexa 488, dextran–Alexa 594, cholera toxin subunit B–Alexa 647, or HRP), 2 mg/mL rat brain cytosol (4), 11.25 mM Hepes at pH 7.0, 1.35 mM magnesium acetate, 0.18 mM DTT, and 45 mM potassium acetate. As an ATP-regenerating system, 3.2 mM ATP, 26 mM creatine phosphate, and

0.132 mg creatine kinase (800 units/mg), or as an ATP-depleting system, 5 μL hexokinase (1,500 units/mL dissolved in 250 mM glucose), were added. The reaction mixtures were incubated for 45 min (unless otherwise stated) at 37 °C with slow agitation, and control reactions were kept on ice. Sorting reactions were carried out in a 50-μL final volume. Five microliters of each reaction were transferred into 1 mL of PBS on coverslips (18 mm diameter) in 12-well plates and centrifuged for 45 min at 5,868 $\times$ *g* at 4 °C. Microscopy and data analysis were performed essentially as described (12); see *SI Methods* for details.

ACKNOWLEDGMENTS. We thank I. Bethani, P. Hoopmann, and H. D. Schmitt for helpful discussions and ideas. We thank R. S. Goody (Max Planck Institute of Molecular Physiology, Dortmund, Germany) for the gift of GDP dissociation inhibitor; U. Winter (Max Planck Institute for Biophysical Chemistry, Göttingen, Germany) for the α-SNAP constructs; and C. Haft, R. Rojas, and J. S. Bonifacino (National Institutes of Health) for the retromer and sorting nexin antibodies. We thank C. Schäfer for technical assistance. S.O.R. thanks A. Bock for excellent assistance. S.V.B. and S.A. acknowledge the support of the MSc/PhD program ''Molecular Biology'' (International Max Planck Research Schools). S.O.R. acknowledges the support of a grant from the German Ministry of Research and Education (Nanolive, ''Vesikelbewegungen durch Nanoauflösung'') and from the Deutsche Forschungsgemeinschaft Research Center for Molecular Physiology of the Brain/Excellence Cluster 171.

1. Mills IG, Jones AT, Clague MJ (1999) Regulation of endosome fusion. *Mol Membr Biol* 16:73–79.
2. Jahn R, Lang T, Sudhof TC (2003) Membrane fusion. *Cell* 112:519–533.
3. Gruenberg J, Howell KE (1989) Membrane traffic in endocytosis: Insights from cell-free assays. *Annu Rev Cell Biol* 5:453–481.
4. Brandhorst D, et al. (2006) Homotypic fusion of early endosomes: SNAREs do not determine fusion specificity. *Proc Natl Acad Sci USA* 103:2701–2706.
5. Stoorvogel W, Oorschot V, Geuze HJ (1996) A novel class of clathrin-coated vesicles budding from endosomes. *J Cell Biol* 132:21–33.
6. Spiro DJ, Boll W, Kirchhausen T, Wessling-Resnick M (1996) Wortmannin alters the transferrin receptor endocytic pathway in vivo and in vitro. *Mol Biol Cell* 7:355–367.
7. Martys JL, et al. (1996) Wortmannin-sensitive trafficking pathways in Chinese hamster ovary cells. Differential effects on endocytosis and lysosomal sorting. *J Biol Chem* 271:10953–10962.
8. Damke H, Baba T, Warnock DE, Schmid SL (1994) Induction of mutant dynamin specifically blocks endocytic coated vesicle formation. *J Cell Biol* 127:915–934.
9. Pagano A, Crottet P, Prescianotto-Baschong C, Spiess M (2004) In vitro formation of recycling vesicles from endosomes requires adaptor protein-1/clathrin and is regulated by rab4 and the connector rabaptin-5. *Mol Biol Cell* 15:4990–5000.
10. Prekeris R, Klumperman J, Chen YA, Scheller RH (1998) Syntaxin 13 mediates cycling of plasma membrane proteins via tubulovesicular recycling endosomes. *J Cell Biol* 143:957–971.
11. Clift-O'Grady L, et al. (1998) Reconstitution of synaptic vesicle biogenesis from PC12 cell membranes. *Methods* 16:150–159.
12. Geumann U, Barysch SV, Hoopmann P, Jahn R, Rizzoli SO (2008) SNARE function is not involved in early endosome docking. *Mol Biol Cell* 19(12):5327–5337.
13. Willig KI, Rizzoli SO, Westphal V, Jahn R, Hell SW (2006) STED microscopy reveals that synaptotagmin remains clustered after synaptic vesicle exocytosis. *Nature* 440:935–939.
14. Bethani I, et al. (2007) The specificity of SNARE pairing in biological membranes is mediated by both proof-reading and spatial segregation. *EMBO J* 26:3981–3992.
15. Wessling-Resnick M, Braell WA (1990) Characterization of the mechanism of endocytic vesicle fusion in vitro. *J Biol Chem* 265:16751–16759.
16. Barnard RJ, Morgan A, Burgoyne RD (1996) Domains of alpha-SNAP required for the stimulation of exocytosis and for N-ethylmalemide-sensitive fusion protein (NSF) binding and activation. *Mol Biol Cell* 7:693–701.
17. Zhao C, Slevin JT, Whiteheart SW (2007) Cellular functions of NSF: Not just SNAPs and SNAREs. *FEBS Lett* 581:2140–2149.
18. Tooze SA, Huttner WB (1990) Cell-free protein sorting to the regulated and constitutive secretory pathways. *Cell* 60:837–847.
19. Itin C, Rancano C, Nakajima Y, Pfeffer SR (1997) A novel assay reveals a role for soluble N-ethylmaleimide-sensitive fusion attachment protein in mannose 6-phosphate receptor transport from endosomes to the trans Golgi network. *J Biol Chem* 272:27737–27744.
20. Lim SN, et al. (2001) Identification of discrete classes of endosome-derived small vesicles as a major cellular pool for recycling membrane proteins. *Mol Biol Cell* 12:981–995.
21. Matsuoka K, et al. (1998) COPII-coated vesicle formation reconstituted with purified coat proteins and chemically defined liposomes. *Cell* 93:263–275.
22. de Wit H, et al. (2001) Rab4 regulates formation of synaptic-like microvesicles from early endosomes in PC12 cells. *Mol Biol Cell* 12:3703–3715.
23. Lichtenstein Y, Desnos C, Faundez V, Kelly RB, Clift-O'Grady L (1998) Vesiculation and sorting from PC12-derived endosomes in vitro. *Proc Natl Acad Sci USA* 95:11223–11228.
24. Arighi CN, Hartnell LM, Aguilar RC, Haft CR, Bonifacino JS (2004) Role of the mammalian retromer in sorting of the cation-independent mannose 6-phosphate receptor. *J Cell Biol* 165:123–133.
25. Popoff V, et al. (2007) The retromer complex and clathrin define an early endosomal retrograde exit site. *J Cell Sci* 120:2022–2031.
26. Miller SE, Collins BM, McCoy AJ, Robinson MS, Owen DJ (2007) A SNARE-adaptor interaction is a new mode of cargo recognition in clathrin-coated vesicles. *Nature* 450:570–574.
27. Miller EA, et al. (2003) Multiple cargo binding sites on the COPII subunit Sec24p ensure capture of diverse membrane proteins into transport vesicles. *Cell* 114:497–509.
28. Mossessova E, Bickford LC, Goldberg J (2003) SNARE selectivity of the COPII coat. *Cell* 114:483–495.
29. Rein U, Andag U, Duden R, Schmitt HD, Spang A (2002) ARF-GAP-mediated interaction between the ER-Golgi v-SNAREs and the COPI coat. *J Cell Biol* 157:395–404.
30. Chidambaram S, Zimmermann J, von Mollard GF (2008) ENTH domain proteins are cargo adaptors for multiple SNARE proteins at the TGN endosome. *J Cell Sci* 121:329–338.
31. Salem N, Faundez V, Horng JT, Kelly RB (1998) A v-SNARE participates in synaptic vesicle formation mediated by the AP3 adaptor complex. *Nat Neurosci* 1:551–556.
32. Backer JM (2000) Phosphoinositide 3-kinases and the regulation of vesicular trafficking. *Mol Cell Biol Res Commun* 3:193–204.
33. McBride HM, et al. (1999) Oligomeric complexes link Rab5 effectors with NSF and drive membrane fusion via interactions between EEA1 and syntaxin 13. *Cell* 98:377–386.
34. Mills IG, Urbe S, Clague MJ (2001) Relationships between EEA1 binding partners and their role in endosome fusion. *J Cell Sci* 114:1959–1965.
35. Simonsen A, Gaullier JM, D'Arrigo A, Stenmark H (1999) The Rab5 effector EEA1 interacts directly with syntaxin-6. *J Biol Chem* 274:28857–28860.
36. Leonard D, et al. (2008) Sorting of EGF and transferrin at the plasma membrane and by cargo-specific signaling to EEA1-enriched endosomes. *J Cell Sci* 121:3445–3458.
37. Peters C, Baars TL, Buhler S, Mayer A (2004) Mutual control of membrane fission and fusion proteins. *Cell* 119:667–678.